



## **Anatomy of the Planarian *Dugesia japonica* I. The Muscular System Revealed by Antisera against Myosin Heavy Chains**

Authors: Orii, Hidefumi, Ito, Hideki, and Watanabe, Kenji

Source: Zoological Science, 19(10) : 1123-1131

Published By: Zoological Society of Japan

URL: <https://doi.org/10.2108/zsj.19.1123>

---

BioOne Complete ([complete.BioOne.org](https://complete.BioOne.org)) is a full-text database of 200 subscribed and open-access titles in the biological, ecological, and environmental sciences published by nonprofit societies, associations, museums, institutions, and presses.

Your use of this PDF, the BioOne Complete website, and all posted and associated content indicates your acceptance of BioOne's Terms of Use, available at [www.bioone.org/terms-of-use](https://www.bioone.org/terms-of-use).

Usage of BioOne Complete content is strictly limited to personal, educational, and non - commercial use. Commercial inquiries or rights and permissions requests should be directed to the individual publisher as copyright holder.

---

BioOne sees sustainable scholarly publishing as an inherently collaborative enterprise connecting authors, nonprofit publishers, academic institutions, research libraries, and research funders in the common goal of maximizing access to critical research.

# Anatomy of the Planarian *Dugesia japonica*

## I. The Muscular System Revealed by Antisera against Myosin Heavy Chains

Hidefumi Orii\*, Hideki Ito and Kenji Watanabe

*Laboratory of Regeneration Biology, Department of Life Science, Graduate School of Science, Himeji Institute of Technology, Harima Science Garden City, Akou-gun, Hyogo 678-1297, Japan*

**ABSTRACT**—The planarian *Dugesia japonica* has two genes encoding myosin heavy chain, *DjMHC-A* and *B* (Kobayashi *et al.*, 1998). We produced antibodies specifically recognizing each myosin heavy chain protein using their carboxyl terminal regions expressed in *E. coli* as antigens. Immunohistochemical analyses of sections and whole-mount specimens revealed the detailed structure and distribution of each type of muscle fiber in the planarian. In general, the MHC-A muscle fibers were distributed beneath the epithelial layers, namely, they were observable in the pharynx, the mouth, the intestine, the eyes and the body wall. In the pharynx, only MHC-A muscle fibers were present. In contrast, the MHC-B muscle fibers were distributed in the mesenchyme as dorso-ventral and transverse muscles, and in the body wall. The body-wall muscles were composed of an outer layer of circular MHC-A muscles and inner longitudinal and intermediate diagonal MHC-B muscle layers. Thus, two types of muscle fibers were distinguished by their distribution in the planarian.

**Key words:** Platyhelminthes, morphology, muscle, evolution, regeneration.

### INTRODUCTION

Freshwater planarians have remarkable regeneration ability. After amputation, a body piece of the planarian can completely regenerate the body as it was. In spite of many studies performed over a long period, it still remained to know in detail about when, where and how the lost cells and tissues reform during planarian regeneration. Anatomical knowledge of planarians at the non-regenerating stage is prerequisite for understanding regeneration mechanisms. Although there have been many histological studies on various species of planarians (Rieger *et al.*, 1991b and literature therein), most histological studies have been performed to compare taxonomic characteristics between species and there are not so many reports on various tissues of a given planarian species with high regeneration ability. In addition, it is not so easy to distinguish certain tissues from the surrounding tissues in planarians by histochemical methods (for example, Pedersen, 1959). For these reasons, we have used tissue-specific markers to perform histological analyses of the intact (non-regenerating) planarian *Dugesia*

*japonica*, which was as a standard animal established in our laboratory to study regeneration mechanisms (Orii *et al.*, 1999). Such studies will provide a morphological basis for understanding the mechanisms of planarian regeneration. Here we performed such a study focusing on the muscular system of this organism.

Several descriptions of the muscular system of planarians at the light and electron microscopic levels have been published (for example, MacRae, 1963; Morita, 1965; Sarnat, 1984). In addition to the conventional methods, phalloidin conjugated with a fluorescent probe has been used for visualizing muscle fibers, and revealed the meshwork structure of the body-wall muscles in various planarians (Reiger *et al.*, 1994; Tyler and Hyra, 1998). In the planarian *Girardia (Dugesia) tigrina*, which is closely related to the *Dugesia japonica* used in this study, Kreshchenko *et al.* (1999) observed the muscular system during pharynx regeneration using tetramethylrhodamine isothiocyanate (TRITC)-phalloidin. Cebria *et al.* (1997) demonstrated that the monoclonal antibody TMUS13, which recognizes myosin heavy chain(s), was useful for visualizing the body-wall muscles. Previously, we showed that the planarian *D. japonica* has at least two genes for myosin heavy chain (*DjMHC-A* and *DjMHC-B*), both of which encode striated muscle type myosins, and that each gene was expressed in distinct cells (Kobayashi *et al.*,

\* Corresponding author: Tel. +81-791-58-0187;  
FAX. +81-791-58-0187.  
E-mail: orii@sci.himeji-tech.ac.jp

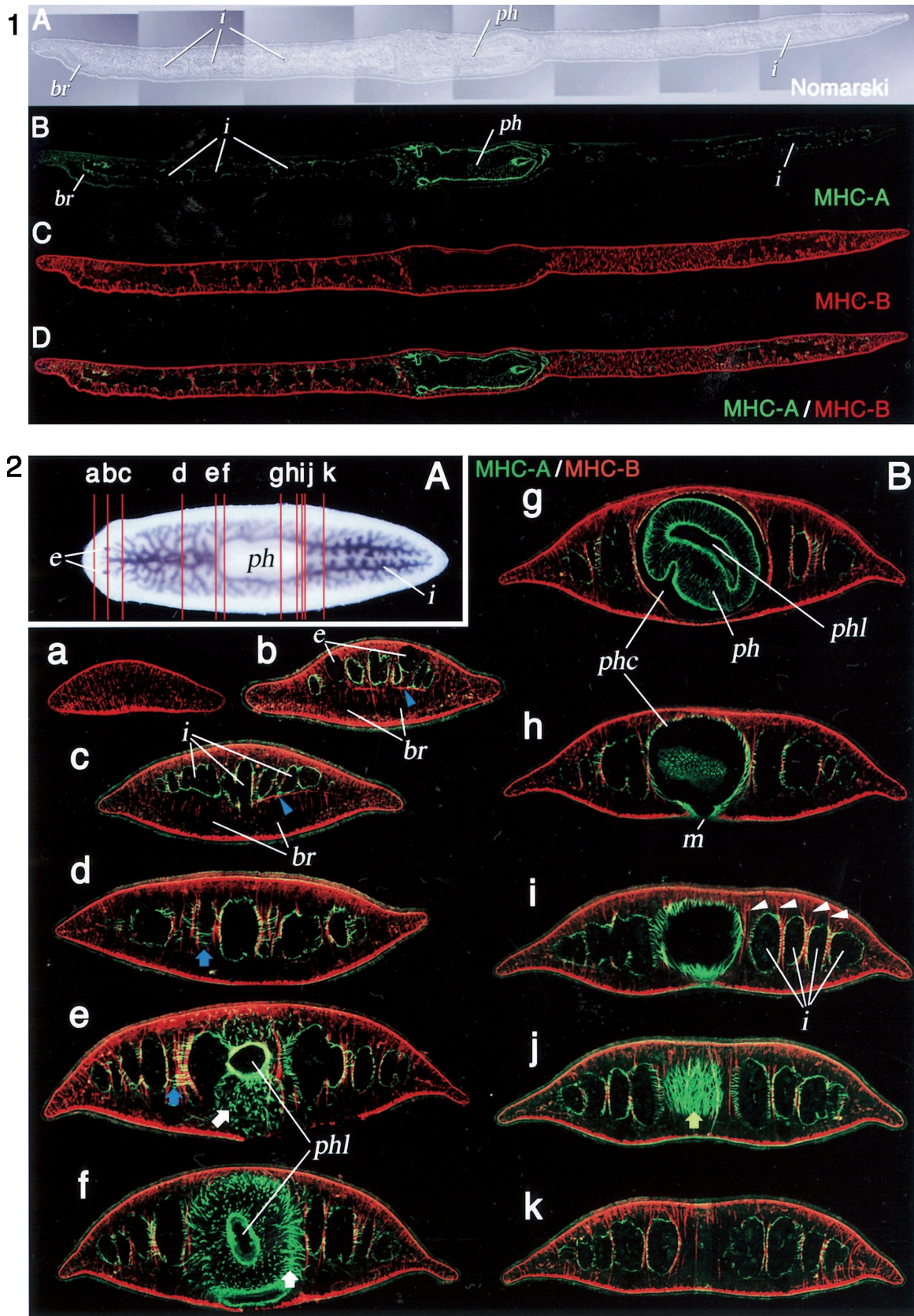


**Fig. 1.** Distribution of MHC-A and B muscles. Sagittal sections. *br*, brain; *i*, intestinal duct; *ph*, pharynx. **(A)** Nomarski image. **(B)** Immunostaining with anti-DjMHC-A (green). **(C)** Immunostaining with anti-DjMHC-B (red). **(D)** Merged image consisting of **(B)** and **(C)**. All images are in the same frame. Anterior on the left, dorsal on the top.

1998). *In situ* hybridization revealed that the *DjMHC-A* gene was expressed at a high level in the pharynx and at a low level in the body wall, whereas the *DjMHC-B* gene was highly expressed in muscles of the body wall and the mesenchyme. These findings suggested that the two types of muscles have distinctive functions. However, the morphology of these muscles in the planarian remained unknown. In this study, we report the muscular structure of the planarian *D. japonica* using antisera against DjMHC-A and B.

## MATERIALS AND METHODS

### Animals

The freshwater planarian *Dugesia japonica*, clonal strain SSP, was used in this study (Ito *et al.*, 2001). The worms were maintained asexually in autoclaved tap water at room temperature (RT, 22–24°C) and fed chicken liver twice a week. Worms about 5 to 10 mm in length were starved for at least 1 week before use.

### Production of antibodies

Based on the deduced amino acid sequences of cDNAs for *DjMHC-A* and *DjMHC-B* (Kobayashi *et al.*, 1998), respective sets of primers were designed. In order to produce antibodies specific to each myosin heavy chain protein, we focused on their carboxyl terminal regions, in which there is low similarity between the two myosins. For DjMHC-A, the cDNA corresponding to the sequence SVSTARGGSMAPGTTTTVKSTLSVSASSRRQSSVSREG of the carboxyl terminus was amplified by polymerase chain reaction (PCR) using forward primer 5'-ATCGTAGATCTGTGTCTACT-3', containing a *Bgl*II site (underlined), and reverse primer 5'-TTT-TAAGCTTATCCTTCTCGT-3', containing a *Hind*III site (underlined). The PCR product was cloned into the pQE40 vector (Qiagen) using these sites. The construct was introduced into *E. coli* strain XL1Blue (Stratagene). The carboxyl terminal region of the DjMHC-A protein was expressed as a fusion protein with dihydrofolate reductase and a histidine tag, and purified using a Ni-NTA resin column according to the manufacturer's protocol (Qiagen). The protein was dialyzed against water, lyophilized, and dissolved in phosphate buffered saline (PBS; KCl 0.2 g, NaCl 8 g, KH<sub>2</sub>PO<sub>4</sub> 0.2 g, Na<sub>2</sub>HPO<sub>4</sub> 12H<sub>2</sub>O 2.9 g per liter). An appropriate volume of this solution was emulsified with Titer Max Gold adjuvant (CytRx) and injected into Balb/c mice or Japanese white rabbits at intervals of 1 month. The antisera were prepared according to a standard method (Harlow and Lane, 1988). For DjMHC-B, forward primer 5'-TCTAGATCTGTAAAC-CGTGGT-3' and reverse primer 5'-AATGTTTTCGAAGCTTTCT-TTA-3' were used for amplification of the cDNA corresponding to the carboxyl terminal region of SVNRGASMGPGTKISITSSRIED. All other procedures for preparation of the antisera against DjMHC-B were same as those for DjMHC-A.

### Immunohistochemistry

Immunohistochemistry of paraffin-embedded sections was performed as described previously (Ito *et al.*, 2001). Antisera against DjMHC-A and DjMHC-B were used at 800-fold dilution as

the primary antibody. The antiserum against *D. japonica* cytochrome *b*<sub>561</sub> was also used for staining of the neural tissue (Asada *et al.*, 2001). Goat anti-mouse IgG antibody conjugated with Cy3 (Jackson Immuno Research Laboratories) and goat anti-rabbit IgG antibody conjugated with Alexa 488 (Molecular Probe) were used as the secondary antibodies. The specimens were counter-stained for nuclei with propidium iodide (0.5 µg/ml) or Hoechst 33342 (0.5 µg/ml) and observed under a fluorescence microscope BX60 (Olympus) or a confocal laser scanning microscope LSM510 (Zeiss).

Immunostaining of whole-mount specimens was also performed. Worms 2–3 mm in length were relaxed in cold 2% HCl in 5/8 Holtfreter's solution (NaCl 2.188 g, KCl 0.031 g, CaCl<sub>2</sub> 0.063 g, NaHCO<sub>3</sub> 0.125 g per liter) for 5 min, fixed in Carnoy's fixative (ethanol:chloroform:acetic anhydride, 6:3:1) at 4°C for 3 hr, and bleached in a 1:5 mixture (vol/vol) of hydrogen peroxide:methanol under fluorescent light at RT overnight. They were hydrated by sequential treatment with 70, 50, and 30% ethanol and PBS containing 0.1% (vol/vol) Triton X-100 (TPBS). After treatment with TPBS supplemented with 10% (vol/vol) goat serum (Gibco) (blocking buffer) at RT for 1 hr, the specimens were incubated at 4°C overnight with the primary antiserum diluted 800-fold with the blocking buffer, and washed several times with TPBS at RT for 1 hr. Then they were treated at 4°C overnight with the secondary antibody diluted 800-fold with the blocking buffer. After the specimens were washed several times with TPBS at RT for 1 hr, they were mounted in 50% glycerol and observed under a confocal laser scanning microscope LSM510 (Zeiss).

## OBSERVATIONS

In order to produce the specific antisera against DjMHC-A or B, we used as antigen the carboxyl terminal region of each protein which was expressed in *E. coli*. The immunostaining patterns using these antisera were corresponded with those of *in situ* hybridization using the gene probes (Kobayashi *et al.*, 1998), demonstrating that the antisera had sufficient specificity to distinguish the two myosin heavy chain proteins (data not shown). We used these antisera for immunostaining with paraffin-embedded sections and whole-mount specimens of the planarian *Dugesia japonica*.

### Distinct distributions of MHC-A and MHC-B muscles

MHC-A muscle fibers were seen in the pharynx, the mouth, the intestine, the body wall and the eyes. In contrast, MHC-B muscle fibers were seen in the body wall and the mesenchyme (Figs. 1 and 2). There were two types of MHC-B muscles in the mesenchyme: 'dorso-ventral muscles' and 'transverse muscles', which could be distinguished by their directions (Figs. 2B and 3B). The dorso-ventral muscles connected the dorsal and ventral body-wall muscles. The

**Fig. 2.** Distribution of MHC-A and B muscles. (A) Dorsal view of a planarian whose intestinal duct was stained with Indian ink (Ito *et al.*, 2001). (B) Immunostaining with anti-DjMHC-A (green) and anti-DjMHC-B (red). a–k show cross sections at the positions indicated by the corresponding red lines in (A). Dorsal is on the top. Blue (in b and c) and white (in i) arrowheads indicate typical examples of the transverse muscle and dorso-ventral muscle fibers, respectively. Blue arrows in d and e indicate MHC-A muscle fibers connecting the neighboring branches of the intestinal duct. White arrows in e and f indicate typical examples of pharynx anchoring muscles. The yellow arrow in j indicates MHC-A muscle fibers beneath the epithelium of the posterior wall of the pharyngeal cavity. br, brain; e, eye; i, intestinal duct; m, mouth; ph, pharynx; phc, pharyngeal cavity; phl, pharyngeal lumen.

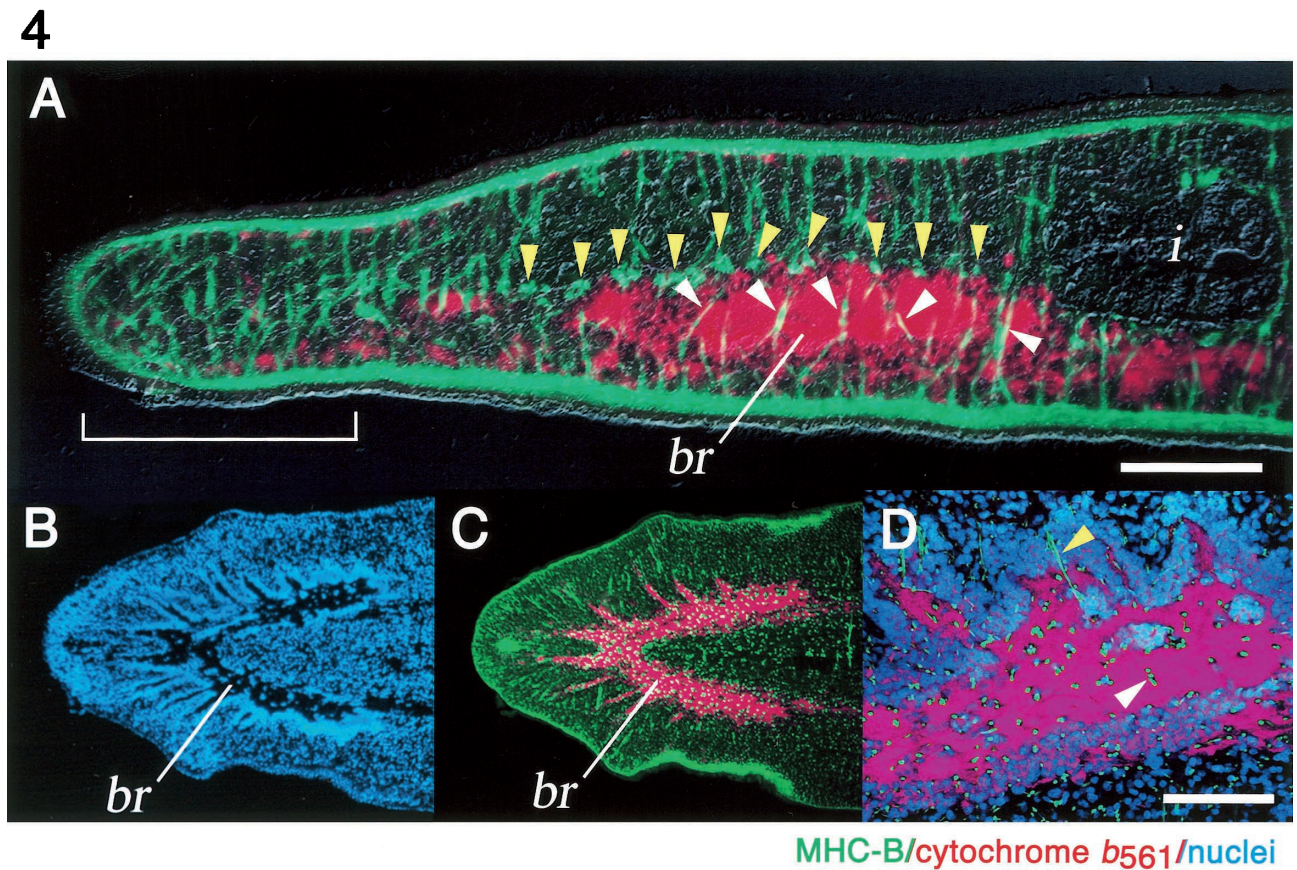
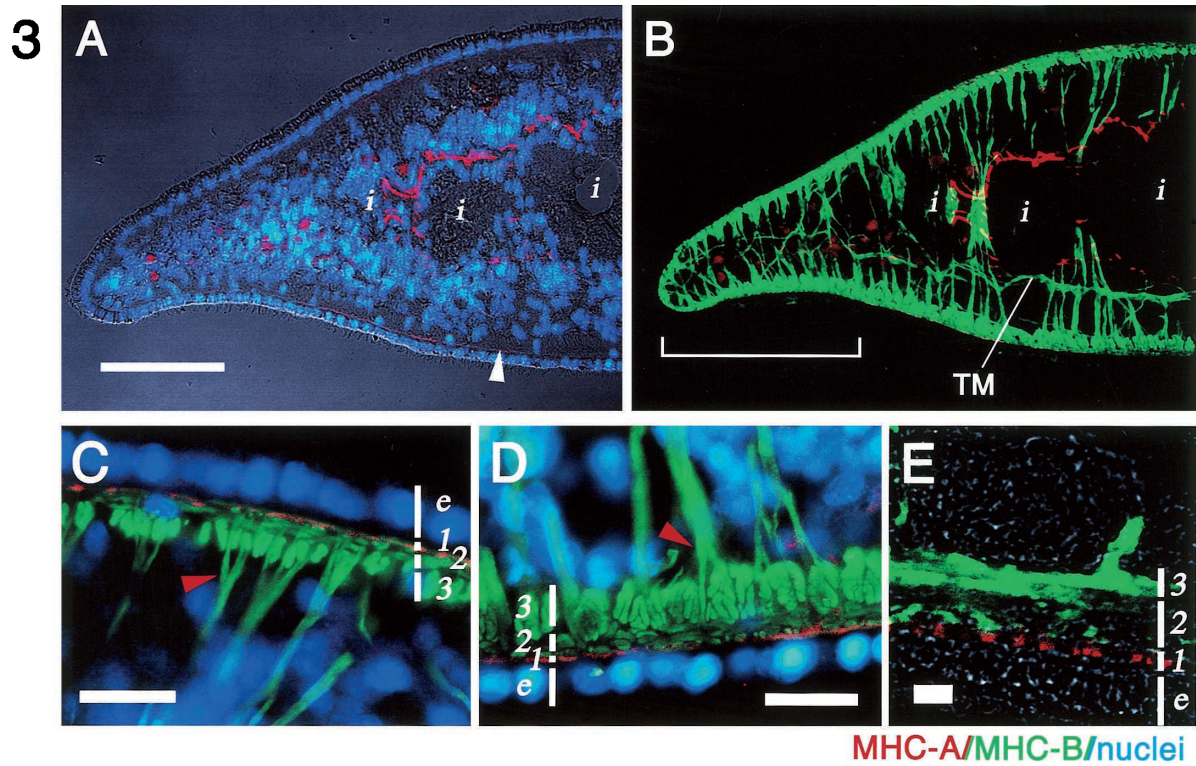


**Fig. 3.** Muscular structure in the intestine and body wall. Sections of the body trunk were triple stained with anti-DjMHC-A (red), anti-DjMHC-B (green) and Hoechst 33342 (for nuclear staining; blue). **(A)–(D)** Cross sections. Dorsal is on the top. **(A)** Staining with anti-DjMHC-A (red) and nuclear staining (blue) are superimposed on the Nomarski image. The white arrowhead indicates the circular muscle fiber of the body wall. **(B)** Images stained with anti-DjMHC-A (red) and anti-DjMHC-B (green) were merged. The frame is same as that in **(A)**. *i*, intestinal duct; TM,

fibers of dorso-ventral muscles were distributed throughout the whole body and ran through the narrow space between the branches of the intestinal duct, which occupied a considerable proportion of the mesenchymal space (see white arrowheads in Fig. 2B for typical examples). In the marginal region of the body, the meshwork structure of the dorso-ventral muscle fibers was observable (brackets in Fig. 3B and Fig. 4A). The transverse muscles were also seen from head to tail, even in the mesenchyme under the pharynx (blue arrowheads in Fig. 5A). Although some transverse-muscle fibers seemed to cross through the body, some seemed to connect the edge with the ventral body-wall muscles or the dorso-ventral muscles (data not shown). All transverse muscles were present only in the ventral side of the intestinal ducts (Figs. 2 and 3B). In general, MHC-A muscle fibers were thinner and more sparsely distributed than MHC-B muscle fibers.

### Body wall

Three layers of body-wall muscles were observable beneath the basement layer of extracellular matrix under the monolayer of epidermal cells (layer e in Fig. 3C–E). Staining of sagittal sections and whole-mount specimens with anti-DjMHC-A and anti-DjMHC-B showed that the outer layer was composed of circular muscle fibers of MHC-A present at regular intervals throughout the body (layer 1 in Fig. 3C–E, Fig. 5C and E). The middle layer was a meshwork composed of MHC-B muscle fibers (layer 2 in Fig. 3C–D, Fig. 5F). The inner layer was composed of longitudinal muscles of MHC-B (layer 3 in Fig. 3C–D, Fig. 5F). Although the dorsal and ventral body-wall-muscle layers had basically the same structures, the ventral layer is thicker than the dorsal one, due to a thicker inner layer of longitudinal MHC-B muscles (Fig. 3C and D). The dorso-ventral muscle fibers branched at their ends, penetrated through the inner longitudinal muscle layer and connected with the middle layer of the body-wall muscles (red arrowheads in Fig. 3C and D). The middle and inner layers of the body-wall muscles in the marginal region were thinner than those in other regions.

### Head

In order to examine the muscular structure in the head region, we performed double-immunostaining with anti-cytochrome  $b_{561}$  antiserum and anti-DjMHC-B serum (Fig. 4). The anti-cytochrome  $b_{561}$  antiserum reacts specifically with

neural tissues, including the brain and ventral nerve cords, probably because cytochrome  $b_{561}$  is involved in synthesis of neuropeptides such as FMRFamide-related peptides (Asada *et al.*, 2002). The planarian brain is a 'U' shaped structure consisting of a neuropil surrounded by neural cell bodies, each of which contains a nucleus (Fig. 4B–D; Sarnat and Netsky, 1985). Double staining revealed that the dorso-ventral muscles were present throughout the brain region as well as the other regions. They penetrated through the brain and connected the dorsal and ventral body walls (white arrowheads in Fig. 4). In the head region, the transverse muscles were present just above the brain and just beneath the intestinal duct (yellow arrowheads in Fig. 4).

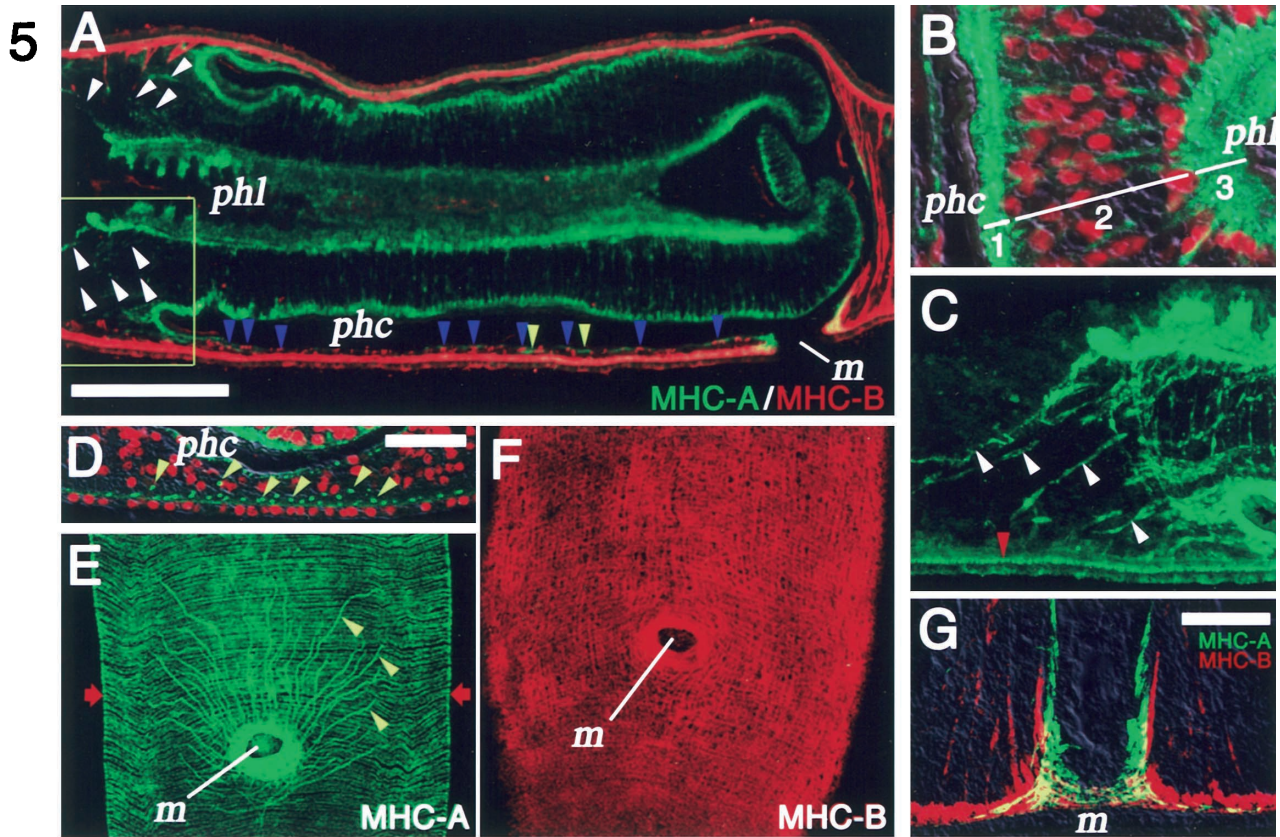
### Pharynx

The pharynx was seen as a cylindrical structure composed of three layers of MHC-A muscle fibers. No MHC-B muscles were present in the pharynx (Figs. 1 and 5A). The outer and inner muscle layers (layers 1 and 3 in Fig. 5B) were seen beneath the epithelial cell layers facing the pharyngeal cavity and pharyngeal lumen, respectively. An intermediate layer between the outer and inner muscle layers contained radial thin muscle fibers connected with both layers (layer 2 in Fig. 5B). As muscle fibers of the outer and inner layers of the pharynx seemed to be more irregular and condensed than those of MHC-A muscles of the body wall, we could not precisely visualize their direction and layered structure under a light microscope. Few nuclei of muscle cells of the outer and inner layers seemed to be located in their respective layers of muscle fibers. Moreover, few nuclei of the epithelial cells facing the pharyngeal lumen were observable in the epithelial layers, as reported previously (Ishii, 1962/63; Asai, 1990).

The epithelial layer surrounding the pharyngeal cavity was lined by a layer of MHC-A muscle fibers (Figs. 2B and 5A). These muscle fibers ran almost longitudinally beneath the epithelial cell layer and they continued to the outer layer of the pharyngeal muscles. Although MHC-B muscle fibers were also seen beneath the layer of MHC-A muscle fibers surrounding the pharyngeal cavity, they must have been derivatives of the dorso-ventral MHC-B muscles. In the base of the pharynx, there were MHC-A muscle fibers connecting the body wall with the outer pharyngeal muscle layer or the inner pharyngeal muscle layer, rather than connecting the outer and inner muscle layers (white arrowheads in Fig. 5A

transverse muscle. The bracket indicates the marginal region where the meshwork structure of MHC-B muscles is seen. (C) Body wall on the dorsal side. (D) Body wall on the ventral side. (E) Confocal image of sagittal section of the ventral body wall. The Nomarski image was superimposed. e, 1, 2 and 3 in (C)–(E) indicate epithelial, outer muscle, middle muscle and inner muscle layers, respectively. Red arrowheads in (C) and (D) indicate branching at the ends of the dorso-ventral muscle fibers. Scale bars in (A), (C), (D) and (E) are 100  $\mu$ m, 20  $\mu$ m, 20  $\mu$ m and 5  $\mu$ m, respectively.

**Fig. 4.** Distribution of MHC-B muscle fibers in the head region. (A) A sagittal section of the head region was stained immunohistochemically with anti-DjMHC-B (green) and anti-cytochrome  $b_{561}$  (red). These images were also superimposed on the Nomarski image. The bracket shows a marginal region where a meshwork structure of MHC-B muscle fibers is seen. Dorsal is on the top. (B) Horizontal section of the head region stained for nuclei with Hoechst 33342. (C) Immunohistochemical staining with anti-DjMHC-B (green) and anti-cytochrome  $b_{561}$  (red). The frame is same as that in (B). (D) High magnification of the brain in a horizontal section stained with anti-DjMHC-B (green), anti-cytochrome  $b_{561}$  (red) and Hoechst 33342 (blue). White arrowheads indicate the dorso-ventral muscle fibers penetrating through the brain. Yellow arrowheads indicate the transverse muscle above the brain. br, brain; i, intestinal duct. Scale bar, about 0.1 mm.



6

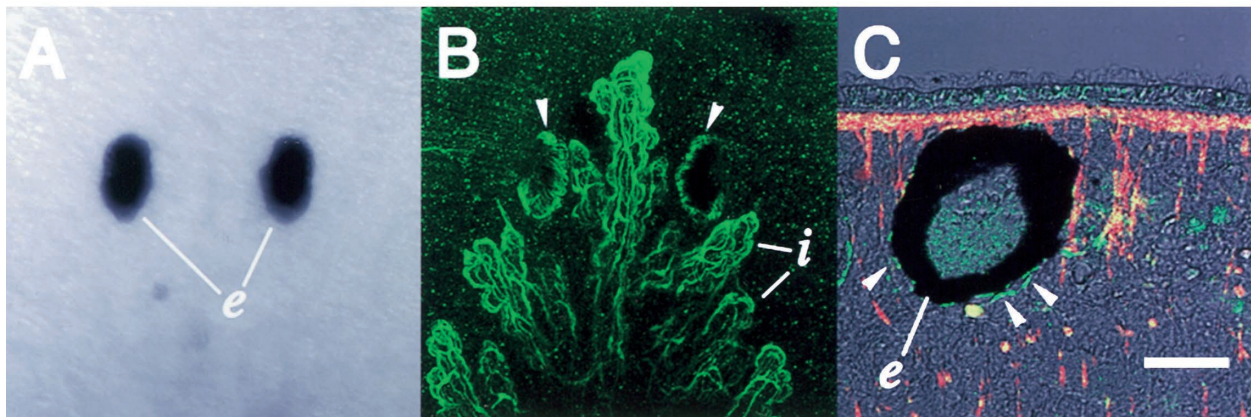


**Fig. 5.** Pharyngeal region and mouth. Immunostaining with anti-DjMHC-A (green). (A) (F) (G) Immunostaining with anti-DjMHC-B (red). (B) (D) (E) Nuclei were stained with propidium iodide (red). (B) (D) (G) The Nomarski image was merged. (A) Sagittal section. Scale bar, about 0.2 mm. (B) High magnification of a cross section of the pharynx. 1, 2 and 3 indicate the outer, intermediate and inner layers of pharyngeal muscles, respectively. (C) High magnification of the base of the pharynx indicated by the box in (A). The red arrowhead indicates the circular muscle layer of the body wall. (D) High magnification of the ventral region under the pharynx in a cross section at the position indicated by red arrows in (E). Scale bar, about 50  $\mu$ m. (E) (F) Confocal laser scanning microscopic images of the mouth region of the whole-mount specimen along the Z-axis. (G) High magnification of a cross section through the mouth. Scale bar, about 50  $\mu$ m. White, blue and yellow arrowheads indicate pharynx anchoring muscles, transverse muscles and dilator muscles, respectively. *m*, mouth; *phc*, pharyngeal cavity; *phl*, pharyngeal lumen.

**Fig. 6.** Eye. (A) (B) Confocal laser scanning microscopic images of the head region of a whole-mount specimen along the Z-axis. Anterior is on the top. (A) Nomarski image. (B) Immunostaining with anti-DjMHC-A (green). The frame is the same as that in (A). (C) Sagittal section of the eye. Merged Nomarski image and images of immunostaining with anti-DjMHC-A (green) and anti-DjMHC-B (red). Arrowheads indicate the MHC-A muscle fibers surrounding the eyecup. Dorsal is on the top. *e*, eye; *i*, intestinal duct. Scale bar, about 0.1 mm.

and C). These MHC-A muscle fibers which radiated from the pharynx (mainly from the inner muscle layer) must correspond to 'pharynx anchoring muscles' which were previ-

ously referred to by Kreshchenko *et al.* (1999) (white arrows in Fig. 2B). The inner layer of MHC-A muscles continued to the muscle fibers surrounding the intestinal duct.

### Mouth

The mouth is a single pore in the pharyngeal cavity opening on the ventral side. It was surrounded by circular muscle fibers of MHC-A. The MHC-A muscle fibers also ran radially from the mouth (yellow arrowheads in Fig. 5A, D and E). The radial muscles that extended to the anterior region were much longer than those extending to other regions. These muscle fibers ran through the narrow mesenchymal space under the pharynx, rather than through the muscle layer of the body wall, and connected to the body-wall muscles of MHC-B at their ends. The rim of the mouth was recognizable as the boundary between the thick body wall and the thin wall of the pharyngeal cavity. The MHC-B muscles at the rim seemed to be derived only from the inner and middle layers of the body wall (Fig. 5G).

### Intestines

The intestinal duct can easily be visualized by feeding planarian with raw chicken liver stained with Indian ink (Fig. 2A). Branches of the intestinal duct extend to the marginal region of the planarian body without overlapping with each other. The intestinal duct was composed of a thick monolayer of epithelial cells containing many vacuoles. Thin MHC-A muscle fibers surrounded the intestinal duct sparsely, irregularly and longitudinally, rather than circularly (Figs. 3A and 6B). MHC-A muscle fibers connecting neighboring branches of the intestinal duct were also seen (blue arrows in Fig. 2B).

### Eyes

The planarian eye is composed of two types of cells, photoreceptor cells and pigmented cells (Kishida, 1967a; Carpenter *et al.*, 1974a). The pigmented cells form an eyecup and the photoreceptor cells project their microvilli to the inside of the cup. The pigmented eyecup was surrounded by several thin fibers of the MHC-A muscles (Fig. 6). These muscle fibers did not appear to be connected to any other muscles.

## DISCUSSION

Previously we demonstrated that the planarian *D. japonica* has two distinct myosin heavy chain genes, *DjMHC-A* and *B* (Kobayashi *et al.*, 1998). In this study, we demonstrated that muscles containing either gene product were distinguished by their distribution and morphology, which allows us to speculate about their functions. In general, MHC-A muscles were seen as thin fibers just beneath the epithelial cell layer and may be involved in fine and peristaltic movement. In contrast, MHC-B muscles were seen as comparatively thick fibers in the body wall and mesenchyme. They must contribute to maintenance of the body shape in addition to rough movement. That is, MHC-B muscles may constitute the framework of the planarian body. This idea appears to be supported by the presence of dorsoventral muscles penetrating through the brain, as if the mus-

cles fix the brain (Fig. 4). Although we do not know if the planarian has other type(s) of myosin heavy chain or not, most muscles appear to contain either MHC-A or MHC-B fibers, as indicated by comparison with previous observations of musculature using the muscle specific monoclonal antibody TMUS-13 (Bueno *et al.*, 1997) and fluorescent probe-conjugated phalloidin (Kreshchenko *et al.*, 1999). It may be necessary to analyze the dissociated muscles to prove our tentative conclusion that there are no muscle cells containing both MHC-A and MHC-B.

The structural features of the body-wall muscles of *D. japonica* were basically the same as those of *Girardia (D) tigrina* previously described by Cebria *et al.* (1997). According to their description, the body-wall muscles of *Girardia (D) tigrina* are composed of four layers from outside to inside: an outer layer of circular muscle fibers, a thin layer of longitudinal muscle fibers, a layer of diagonal muscle fibers and an inner layer of longitudinal muscle fibers. In *D. japonica*, we could distinguish at least three layers of body-wall muscles: an outer layer of circular fibers, an inner layer of longitudinal fibers and a layer of diagonal and longitudinal fibers between them (Figs. 3 and 5). The pattern of body-wall musculature has been studied in the turbellarians, especially in members of Acoela, because it is useful as a taxonomic character (Tyler and Hyra, 1998). A three-layered structure of the body-wall muscles is widely seen in the turbellarians (Rieger *et al.*, 1991b). Interestingly, an outer layer of circular muscle fibers seems to be common among various species of Platyhelminthes, including parasitic flatworms. In contrast, the inner and intermediate layers seem to be variable. For example, in the trematode *Fasciola hepatica*, the outer, intermediate and inner layers of the body-wall muscles are composed of circular, longitudinal and diagonal muscle fibers, respectively (Mair *et al.*, 1998). In this study, we demonstrated that the outer layer was composed of circular muscle fibers of MHC-A, whereas the other layers of the body wall were composed of MHC-B muscle fibers. This appears to support the idea that the diagonal muscle fibers are derived from the longitudinal muscle layer (Westblad, 1949, cited in Rieger *et al.*, 1991a), rather than from the circular muscle layer (Riser 1987, cited in Rieger *et al.*, 1991a). Although we do not know if a single circular muscle cell forms a complete ring surrounding the body, we suspect that several spindle-shaped-muscle fibers overlapping at their ends form such a ring, based on observations of another turbellarian *Uras-toma cyprinae* (Hooge and Tyler, 1999).

Questions have been raised about the relationship between the body wall and the intestinal duct, which is connected to the body wall (reviewed in Rieger *et al.*, 1991b). The terminus of the intestinal duct at the mouth is expected to have longitudinal and circular muscles if it originates from invagination of the body wall. In most turbellarians without a well-developed pharynx, some circular body-wall-muscle fibers turn into the mouth and contribute to the longitudinal musculature of the duct (Rieger *et al.*, 1994; Hooge and Tyler, 1999). In this study, we showed



molecular evidence for a relationship between the circular body-wall muscles and the pharyngeal muscles, that is, both muscles contain only MHC-A.

Kobayashi *et al.* (1998, 1999) referred to *DjMHC-A*-expressing cells in the mesenchymal region around the base of the pharynx as 'pharynx-forming muscles' or 'pharynx-muscle-forming cells' which were differentiating and migrating into the pharynx. However, these MHC-A muscle fibers obviously connect the pharynx with the body wall in the intact organism, suggesting that they function to fix and pull the pharynx rather than consist of cells that differentiate into pharyngeal muscles (Figs. 2 and 5). Kreshchenko *et al.* (1999) also observed these muscles in *Girardia (D) tigrina* with TRITC-conjugated phalloidin and referred to them as 'anchoring muscles'. In *Macrostomum hystricinum marinum*, which has a simple structured pharynx in the boundary between the body wall and the intestine, Rieger *et al.* (1994) found transverse muscles connecting the body wall and the pharynx. Muscles such as the 'pharynx-anchoring muscles' in *Dugesia* may be seen widely in turbellarians.

Previously, we showed by *in situ* hybridization that during pharyngeal cavity formation, *DjMHC-A*-expressing cells were accumulated and *DjMHC-B*-expressing cells disappeared in the nascent mouth. This suggested that these muscle cells had distinctive functions there (Kobayashi *et al.*, 1998). In the intact mouth, MHC-A muscle fibers form sphincter-like and dilator-like muscles running circularly and radially, respectively, and also line the epithelial layer of the pharyngeal cavity (Fig. 5). In contrast, MHC-B muscle fibers in the mouth seemed to be derived from the body-wall muscle and the dorso-ventral muscles. The morphology of the muscle fibers in the digestive system seems to be very reasonable considering their function. When a planarian eats food, it projects its pharynx outside. Then the body-wall muscles and the sphincter-like muscles around the mouth must be relaxed and the dilator-like muscles must contract, resulting in pulling the rim to open the mouth. Contraction of the MHC-A muscles beneath the epithelial layer of the pharyngeal cavity must result in projection of the pharynx. In addition, regulated contraction of the anchoring muscles may help to project the pharynx in the right direction. The muscular structure of the pharynx, in which radial muscles connect the outer and inner muscles, also seems to be suitable for the flexible movements involved in sucking and swallowing food materials. The digested foods must be transported into every branch of the intestinal duct by coordinated peristaltic contraction of the intestinal MHC-A muscle fibers.

It has been reported that the pigmented eyecup wrapped by a non-cellular fibrous capsule is surrounded by muscle fibers in the marine flatworm *Notoplana acticola* (MacRae, 1966) and the freshwater planarian *Dugesia dorotocephala* (Carpenter *et al.*, 1974a). Also in *D. japonica*, the pigmented eyecup was surrounded by thin muscle fibers of MHC-A (Fig. 6). The lack of connection of these eye-muscle fibers to any other tissues such as the body wall suggests

that the muscle fibers regulate the volume rather than the direction of the eye. In this regard, it is very interesting that morphological changes of microvilli of the photoreceptor cells (Carpenter *et al.*, 1974b) and changes of the extracellular volume inside the eyecup may depend on the light conditions (Azuma, 1997). These changes may be regulated by contraction of the eye-muscle fibers.

In freshwater planarians, the eye, including the pigmented eyecup, is differentiated from neoblasts in the mesenchyme, rather than formed by invagination of the epithelial tissue during regeneration (Kishida, 1967b). However, it has been suggested that the pigmented eyecup is an epithelial tissue, because of the presence of a kind of basal lamina referred to as a 'fibrous capsule' and septate desmosomes between the pigmented cells (Carpenter *et al.*, 1974a). In addition, the pigmented eyecup is surrounded by MHC-A muscle fibers (Fig. 6). It should also be noted that the eyes are formed in the mesoderm by invagination of the ectodermal epithelial layer during embryogenesis in the marine flatworm *Notoplana humilis* (Kato, 1940). These facts appear to support the idea that the pigmented eyecups originated evolutionarily from the epithelial tissue.

To date, histological analyses of diverse species of Platyhelminthes have been performed for reasons of phylogenetic interest. However, it is also necessary to perform histological analyses within a given planarian species in order to characterize it for use as an experimental animal for regeneration studies. In this study, we demonstrated that two types of planarian muscles were distinctive in their distribution and morphology, a conclusion that could not be drawn based on previous *in situ* hybridization analyses (Kobayashi *et al.*, 1998). These studies will provide a structural basis for detailed understanding of the mechanisms of planarian regeneration.

## ACKNOWLEDGEMENTS

We are grateful to Drs. T. Sakurai (Fukushima Biomedical Institute of Environmental and Neoplastic Disease) and M. Dan for fruitful discussions and Dr. A. Tazaki for his reading of the manuscript. We also thank Drs. K. Agata and C. Kobayashi (RIKEN Center for Developmental Biology) and members of our laboratory for their support. This work was supported in part by a Grant-in-Aid (Bio Design Program) from the Ministry of Agriculture, Forestry and Fisheries of Japan, to H.O..

## REFERENCES

- Asada A, Kusakawa T, Orii H, Agata K, Watanabe K, Tsubaki M (2002) Planarian cytochrome *b<sub>561</sub>*: Conservation of a six transmembrane structure and localization along the central and peripheral nervous system. *J Biochem* 131: 175–182
- Asai E (1990) The behavior of pharyngeal outer epithelial cells during regeneration of the planarian *Dugesia japonica japonica*. *J Morphol* 206: 313–325
- Azuma K (1997) Light-induced changes of extracellular volume in a planarian ocellus. *Comp Biochem Physiol* 117A: 155–159
- Bueno D, Baguña J, Romero R (1997) Cell-, Tissue-, and position-specific monoclonal antibodies against the planarian *Dugesia*

- (*Girardia tigrina*). Histochem Cell Biol 107: 139–149
- Carpenter KS, Morita M, Best JB (1974a) Ultrastructure of the photoreceptor of the planarian *Dugesia dorotocephala*. I. Normal eye. Cell Tissue Res 148: 143–158
- Carpenter KS, Morita M, Best JB (1974b) Ultrastructure of the photoreceptor of the planarian *Dugesia dorotocephala*. II. Changes induced by darkness and light. Cytobiologie 8: 320–338
- Cebria F, Vispo M, Newmark P, Bueno D, Romero R (1997) Myocyte differentiation and body wall muscle regeneration in the planarian *Girardia tigrina*. Dev Genes Evol 207: 306–316
- Harlow E, Lane D (1988) Antibodies: A laboratory manual. Cold Spring Harbor Laboratory Press, New York
- Hooge MD, Tyler S (1999) Musculature of the facultative parasite *Urastoma cyprinae* (Platyhelminthes). J Morphol 241: 207–216
- Ishii S (1962/63) Electron microscopic observations on the planarian tissues I. A survey of the pharynx. Fukushima J Med Sci 9–10: 51–73
- Ito H, Saito Y, Watanabe K, Orii H (2001) Epimorphic regeneration of the distal part of the planarian pharynx. Dev Gene Evol 211: 2–9
- Kato K (1940) On the development of some Japanese polyclads. Jpn J Zool 8: 537–573
- Kishida Y (1967a) Electron microscopy studies on the planarian eye I. Sci Rep Kanazawa Univ 12: 75–110
- Kishida Y (1967b) Electron microscopy studies on the planarian eye II. Sci Rep Kanazawa Univ 12: 111–142
- Kobayashi C, Kobayashi S, Orii H, Watanabe K, Agata K (1998) Identification of two distinct muscles in the planarian *Dugesia japonica* by their expression of myosin heavy chain genes. Zool Sci 15: 861–869
- Kobayashi C, Watanabe K, Agata K (1999) The process of pharynx regeneration in planarians. Dev Biol 211: 27–38
- Kreshchenko ND, Reuter M, Sheiman IM, Halton DW, Johnston RN, Shaw C, Gustafsson MKS (1999) Relationship between musculature and nervous system in the regenerating pharynx in *Girardia tigrina* (Plathelminthes). Invert Reprod Dev 35: 109–125
- MacRae EK (1963) Observation on the fine structure of pharyngeal muscle in the planarian *Dugesia tigrina*. J Cell Biol 18: 651–662
- MacRae EK (1966) The fine structure of photoreceptors in a marine flatworm. Z Zellforsch 75: 469–484
- Mair GR, Maule AG, Shaw C, Johnston CF, Halton DW (1998) Gross anatomy of the muscle systems *Fasciola hepatica* as visualized by phalloidin-fluorescence and confocal microscopy. Parasitology 117: 75–82
- Morita M (1965) Electron microscopic studies on planaria. I. Fine structure of muscle fiber in the head of the planarian *Dugesia dorotocephala*. J Ultrastruct Res 13: 383–395
- Orii H, Kato K, Umesono Y, Sakurai T, Agata K, Watanabe K (1999) The planarian HOM/HOX homeobox genes (*Plox*) expressed along the antero-posterior axis. Dev Biol 210: 456–468
- Pedersen KJ (1959) Cytological studies on the planarian neoblast. Z Zellforsch 50: 799–817
- Rieger R, Salvenmoser W, Legniti A, Reindl S, Adam H, Simonsberger P, Tyler S (1991a) Organization and differentiation of the body-wall musculature in *Macrostomum* (Turbellaria, Macrostromidae). Hydrobiologia 227: 119–129
- Rieger RM, Tyler S, Smith III JPS, Rieger G (1991b) Platyhelminthes: Turbellaria. In “Microscopic anatomy of invertebrates Vol. 3. Platyhelminthes and nemertinea” Ed by FW Harrison and BJ Bogitsh, Wiley-Liss, New York, pp 7–140
- Rieger RM, Salvenmoser W, Legniti A, Tyler S (1994) Phalloidin-rhodamine preparations of *Macrostomum hystricinum* marinum (Plathelminthes): morphology and postembryonic development of the musculature. Zoomorphology 114: 133–147
- Riser NW (1987) *Nemertinoidea elongatus gen.n.sp.n.* (Turbellaria: Nemertodermatida) from coarse sand beaches of the western North Atlantic. Proc Helminthol Soc Wash 54: 60–67
- Sarnat HB (1984) Muscle histochemistry of the planarian *Dugesia tigrina* (Turbellaria: Tricladida): implications in the evolution of muscle. Trans Am Microsc Soc 103: 284–294
- Sarnat HB, Netsky MG (1985) The brain of the planarian as the ancestor of the human brain. Can J Neurol Sci 12: 296–302
- Tyler S, Hyra GS (1998) Patterns of musculature as taxonomic characters for the Turbellaria Acoela. Hydrobiologia 383: 51–59
- Westblad E (1949) On *Meara stichopi* (Bock) Westblad, a new representative of Turbellaria Archoophora. Ark Zool Ser 2 1: 43–57

(Received June 24, 2002 / Accepted August 8, 2002)